224 the deletion of *Pten* augmented the phosphorylation of Akt in the corresponding regions
225 of the epithelia in the *Pten* CKO mice (Fig. 7E-H).
226 The stratified and keratinized vagina of control mice administrated with E2
227 expressed Pten predominantly in the basal cells as well (See Fig. 1A). Concomitantly,
228 phospho-Akt was detected in the lower layers of epithelia including basal cells in the
229 control (Fig. 7I) and was augmented throughout the epithelium, particularly in the basal
230 to suprabasal cell layers in the *Pten* CKO mice (Fig. 7J). Intriguingly, in the OVX
231 control mice, Pten was exclusively expressed in the suprabasal cells (See Fig. 1B). The
232 phosphorylated Akt was not detected in the OVX control mice (Fig. 7K). When *Pten*
233 was deleted, phospho-Akt was found in the suprabasal cells but not in the basal cells
234 (Fig. 7L). Thus, Pten expression and its regulation of Akt in the mouse vagina depend
235 on the presence or absence of estrogen, and this might explain the unique phenotypes of
236 the *Pten* CKO mouse vagina.
237

Discussion

Estrogens play a central role in female reproductive organ biology. Despite the importance of this organ system for fertility and women's health, the signaling pathways that regulate cell proliferation and differentiation remain poorly understood. *Pten* tumor-suppressor gene lipid phosphatase activity acts in opposition to PI3K function and *Pten* loss-of-function mutations frequently result in sporadic and hereditary cancers accompanied by Akt activation [1, 4, 30]. Akt was shown to be phosphorylated as a result of estrogen treatment and was described as a functional mediator of estrogen-induced cell proliferation and differentiation in mouse uterus and vagina [9, 31]. Therefore, Akt signaling is currently thought to be an essential mediator for estrogen-induced events. If this is the case, activation of Akt, *per se*, should result in cell proliferation and squamous differentiation in the mouse vaginal epithelium even in the absence of estrogen. To test this hypothesis, we utilized an epithelial cell-specific conditional *Pten* knock-out mice.

First, we expected cell proliferation and squamous hyperplasia in the vaginal epithelium, because *Pten* mutation results in squamous hyperplasia and tumor formation in other stratified and squamous tissues such as skin, esophagus and stomach [1]. Despite the intrinsic similarity among such differentiated stratified, squamous epithelia, the phenotypes observed in the *Pten* CKO mouse vagina are unique. Cell proliferation in the *Pten* CKO mouse vaginal epithelium is indeed increased, however, a remarkable hyperplasia was observed in the suprabasal cells accompanied with abnormal mucin production. Based on the CK1, CK8 and p63 expression pattern, the suprabasal cells in the *Pten* CKO mice are maintained in a largely undifferentiated condition. We infer that the suprabasal cells in the *Pten* CKO mice fail to completely differentiate into squamous

cells and retain an undifferentiated status with the potential for cell proliferation. Immunohistochemical analysis in OVX control mouse vaginae revealed the unique expression of *Pten* in the suprabasal layers. Hence, the primary role for Pten in the mouse vagina seems to block aberrant cell proliferation in the suprabasal cells rather than to control basal cell proliferation in the absence of estrogen.

It was unknown whether the vaginae in the OVX *Pten* CKO mouse develop tumors. It has been reported that 90% of OVX *Pten* heterozygote mice developed uterine epithelial hyperplasia [32]. This suggests that *Pten* loss-of-function is sufficient for the development of complex atypical hyperplasia (CAH) in the absence of estrogen. Since CAH often precedes endometrial carcinoma [32], this may be consistent with a role for *Pten* in vaginal cancers. Therefore, we could not exclude the possibility of spontaneous tumorigenesis in the *Pten* CKO mouse vagina without estrogenic stimulation. Several lines of epithelial cell-specific *Pten* mutants have shown decreased survival rate with severe growth retardation and developments of multiple disorders as age progressed [1, 30]. Further experiments using alternative conditional *Pten* knock-out mice with Cre expression restricted to the vaginal epithelium and higher survivorship will be required to address this issue.

Pten expression shifts from the suprabasal layer to the basal layer upon estrogen administration as was observed in other stratified and squamous tissues. Ours is the first demonstration of an estrogen-dependent role for Pten. Pten appears to regulate cell proliferation in the basal layer to prevent squamous hyperplasia and/or tumors in the presence of estrogens. In addition, prolonged E2 exposure induced invagination of the vaginal epithelium into underlying stroma in the mutants, which phenotypes are associated with vaginal and cervical cancer [33, 34]. Thus, once epithelial

286 cells undergo squamous differentiation, Pten could also function as a tumor suppressor
287 in the vagina. Intriguingly, the p63 expressing region is extended apically in the *Pten*
288 CKO mice. P63 is a marker for basal cell characteristics and is associated with
289 proliferative capacity in the stratified epithelium. Activation of Akt induces increase of
290 p63 expression and is associated with transformation of keratinocytes [35].
291 Our mouse model revealed several downstream effectors of PI3K/Akt in the
292 mouse vagina. One of the targets is mTOR, which showed increased phosphorylation
293 levels together with Akt phosphorylation resulting from *Pten* deletion. mTOR regulates
294 translation and cell growth as a central component of raptor (mTORC1) or rictor
295 (mTORC2) complexes via phosphorylation of their substrates (e.g., p70 ribosomal S6
296 kinase and 4E binding protein). The PI3K/Akt/mTOR pathway also represents a
297 proliferative pathway activated by PI3K and Pten loss, and contributes to the formation
298 of multiple tumor types [30, 36]. Notably, tumors involving *Pten* deletions or Akt
299 activations are highly sensitive to a specific inhibitor of mTOR, rapamycin [37, 38]. In our
300 mouse model, levels of cell proliferation, particularly in the suprabasal layers, were
301 decreased by rapamycin treatment, accompanied with partial rescue of their hyperplasia,
302 supporting a role for the Akt/mTOR pathway in the mutant phenotypes. Rapamycin
303 treatment clearly diminished cell proliferation although, mucin production in suprabasal
304 layer cells was retained. This supports the involvement of an additional alternative
305 pathway for such abnormal cell differentiation. We found MAPK activation in the
306 suprabasal cells in the mutant mouse vagina and activation of ERK1/2 has been
307 implicated for mucin production in respiratory tract, intestine and prostate [24-26]. This
308 supports a model wherein aberrant mucin production results from misactivation of the
309 MAPK pathway.

Among vaginal carcinoma, approximately 80% are squamous cell carcinomas, with 13% being adenocarcinoma [39]. There are a number of types of vaginal adenocarcinoma reported, including clear cell, serous and mucinous types [40-42]. The histogenesis of primary vaginal adenocarcinoma, particularly which is not associated with *in utero* DES exposure [43], is not well understood. The current results suggest a contribution of the Pten/Akt/mTOR signaling pathway to the aforementioned histogenesis; in particular, the vaginal mucinous adenocarcinoma might be involved in MAPK signaling cascade as well. In addition, this study also showed that vaginal phenotypes in the *Pten* CKO mice depend on the estrogen levels. It is currently thought that excess estrogen stimulation plays a role in the etiology of hyperplasia and/or tumors in female reproductive organs. However, even in the absence of estrogen, *Pten* mutation induced a deleterious effect on mouse vagina. Taken together, the results presented herein have important implications for treatment of lesions in the reproductive organ in women.

Pten plays a critical role in epithelial cell homeostasis and acts as a tumor suppressor in various tissues. Here we took advantage of unique features of the mouse vagina as a model for analyzing the role of Pten in epithelial cell homeostasis. In the absence of estrogen, Pten is expressed in the suprabasal cells where it inhibits ectopic cell proliferation (Fig. 8A). In the presence of estrogen, Pten functions in the basal cells where it may prevent excessive cell proliferation (Fig. 8B). Thus, Pten is indispensable for homeostasis in the vaginal epithelium where its function depends on estrogen levels. This provides new insight into the role of Pten in tissue homeostasis.

Conflict of interest

334 The authors declare no conflict of interest.

335

336 **Acknowledgements**

337 We would like to thank Dr. J. Takeda, Osaka University, Japan, for providing
338 *K5-Cre* mice. We also thank Dr. Y. Mikami, Kyoto University, Japan and Dr. Bruce
339 Blumberg, University of California, Irvine, for their support. This study was supported
340 by Grant-in-Aid for Young Scientists B, Grant-in-Aid for Scientific Research B from
341 the Ministry of Education, Culture, Sports, Science and Technology of Japan, and
342 Health Sciences Research Grant from the Ministry of Health, Labour and Welfare,
343 Japan.

344

345 **Materials and Methods**

346 *Mouse and chemical treatment*

347 C57BL/6J (CLEA, Tokyo, Japan), *K5-Cre* [44], and *Pten*-floxed mice [45] were
348 maintained under 12 h light/12 h dark at 23-25°C and fed laboratory chow (CA-1,
349 CLEA) and tap water *ad libitum*. *K5-Cre* line (B6 background) and *Pten*-floxed line
350 ($Pten^{flox\,flox}$; 129 background) were crossed to produce male *K5Cre/+*;$Pten^{flox\,+}$ mice.
351 *Pten* CKO mice (*K5Cre/+*;$Pten^{flox\,flox}$) were obtained by crossing *K5Cre/+*;$Pten^{flox\,+}$
352 male mice and $Pten^{flox\,flox}$ female mice. Cre-negative and $Pten^{flox\,flox}$ siblings were used
353 as control. In such conditions, no prominent phenotypic variation was observed within
354 each experimental group. In most experiments, mice were ovariectomized (OVX) at 6
355 weeks of age and sacrificed at 8 weeks of age. For examining effects of estrogen, a
356 single injection of 0.1 μg 17β-estradiol (E2) (Sigma, St. Louis, MO, USA) was given to
357 OVX mice for 3 days and sacrificed 24 h after the last injection. This timing is
358 sufficient to induce stratified and fully keratinized epithelium in the mouse vagina. For
359 a long treatment, OVX mice were implanted with E2 pellets (0.01mg/ pellet, 2 months;
360 Innovative Research of America, Sarasota, FL, USA) into subcutaneous tissue for 2
361 months. Rapamycin (Toronto Research Chemicals, North York, Canada) was
362 reconstituted in DMSO at 10mg/ml then diluted in saline containing 5% PEG400
363 (Sigma) and 5% Tween-80 (Sigma). OVX mice were administrated rapamycin (1 mg/kg
364 body weight/day, i.p.) for 3 weeks. All procedures and protocols were approved by the
365 institutional animal care and use committee at the National Institute for Basic Biology.
366
367 *Histology and immunohistochemistry*
368 Hematoxylin and eosin staining was performed by a standard procedure. PAS

and Alcian blue staining was performed with PAS staining kit (Muto Chemical, Tokyo Japan) and acidic Alcian blue. For immunohistochemistry, paraformaldehyde-fixed, paraffin-embedded sections were incubated with the following primary antibodies: estrogen receptor α (ERα) (H184, 1:200), p63 (4A4, 1:200, Santa Cruz, Santa Cruz, CA), CK8 (1:50, Progen, Heidelberg, Germany), CK1 (1:500), CK14 (1:1000, Covance, Emeryville, CA, USA), Pten (138G6, 1:100), phospho-Akt (D9E, 1:100), phospho-MEK (D26, 1:160) and phospho-ERK1/2 (D13.14.4E, 1:400, Cell Signaling, Danvers, MA, USA). The sections were stained with the Vectastain ABC Kit (Vector Laboratories, Burlingame, CA, USA). Immunofluorescence analysis was performed with Alexa Fluor protein-conjugated secondary antibodies (Life Technology, Carlsbad, CA, USA). For BrdU-immunostaining, mice were injected with BrdU (Sigma) at 100 mg/kg body weight. One hour after the injection, tissues were collected. BrdU-incorporated cells were detected with anti-BrdU antibody (1:20, Roche, Mannheim, Germany). TUNEL assay for the detection of apoptotic cells was performed with the *in situ* apoptosis detection kit (Roche). More than 5 animals were used for each histological analysis. Error bars represent the standard error.

Quantitative RT-PCR

Total RNA (2.5 μg), isolated with an RNeasy kit (Qiagen, Velno, Netherlands) from each group, was used in RT-PCR reactions carried out with SuperScript III reverse transcriptase and SYBR Green Master Mix (Life Technologies) according to manufacturer's instructions. PCR conditions and sequences of primer sets are given in previous report [8]. Relative RNA equivalents for each sample were obtained by standardization of ribosomal protein L8 levels. More than 3 pools of samples per group

were run in triplicate to determine sample reproducibility. Error bars represent the standard error, with all values represented as fold change compared to the control treatment group normalized to an average of 1.0.

Protein Preparation and Immunoblotting

Isolated mouse vaginae were homogenized in buffer [20 mM HEPES, 2 mM EDTA, 2 mM EGTA, 100 mM β-glycerophosphate, 250 mM NaCl, 1% TritonX-100, protease inhibitor cocktail (Roche) and phosphatase inhibitor cocktail (Roche), pH 7.5] and spun at 15,000 rpm for 10 min. The supernatant was collected and protein content was determined using the Bradford Assay (BioRad, Hercules, CA, USA). Proteins (10 μg) were electrophoresed on SDS-polyacrylamide gels and transferred onto a nitrocellulose membrane. The membranes were incubated with the following primary antibodies at a dilution of 1:1000 over night at 4°C: ERα (H184, Santa Cruz), phospho-ERαs (2514 and 2515), mTOR (7C10), phospho-mTOR (D9C2), Akt (C67E7), phospho-Akt (C31E5E and D9E, Cell Signaling). Signals were detected with the ECL prime kit (GE Healthcare, Buckinghamshire, UK). Digital images were taken and densitometry analysis was performed using the NIH Image J software, down loaded from http://rsbweb.nih.gov/ij/. More than 3 pools of samples per group were used.

Statistical analysis

For BrdU-labeling and apoptotic indices, and gene expression analyses, statistical analyses were performed using Student's *t*-test or Welch's *t*-test followed by F-test; differences with $p<0.05$ were considered significant.

References

1 Suzuki A, Itami S, Ohishi M, Hamada K, Inoue T, Komazawa N *et al.* Keratinocyte-specific Pten deficiency results in epidermal hyperplasia, accelerated hair follicle morphogenesis and tumor formation. Cancer Res 2003; 63: 674-681.

2 Blanco V, Keochgerian V. Cowden's syndrome. Case report, with reference to an affected family. Med Oral Patol Oral Cir Bucal 2006; 11: E12-16.

3 Leao JC, Batista V, Guimaraes PB, Belo J, Porter SR. Cowden's syndrome affecting the mouth, gastrointestinal, and central nervous system: a case report and review of the literature. Oral Surg Oral Med Oral Pathol Oral Radiol Endod 2005; 99: 569-572.

4 Yoo LI, Liu DW, Le Vu S, Bronson RT, Wu H, Yuan J. Pten deficiency activates distinct downstream signaling pathways in a tissue-specific manner. Cancer Res 2006; 66: 1929-1939.

5 Buchanan DL, Kurita T, Taylor JA, Lubahn DB, Cunha GR, Cooke PS. Role of stromal and epithelial estrogen receptors in vaginal epithelial proliferation, stratification, and cornification. Endocrinology 1998; 139: 4345-4352.

6 Cooke PS, Buchanan DL, Young P, Setiawan T, Brody J, Korach KS *et al.* Stromal estrogen receptors mediate mitogenic effects of estradiol on uterine epithelium. Proc Natl Acad Sci U S A 1997; 94: 6535-6540.

7 Nelson KG, Sakai Y, Eitzman B, Steed T, McLachlan J. Exposure to diethylstilbestrol during a critical developmental period of the mouse reproductive tract leads to persistent induction of two estrogen-regulated genes. Cell Growth Differ 1994; 5: 595-606.

8 Miyagawa S, Katsu Y, Watanabe H, Iguchi T. Estrogen-independent activation of erbBs signaling and estrogen receptor alpha in the mouse vagina exposed neonatally to diethylstilbestrol. Oncogene 2004; 23: 340-349.

9 Miyagawa S, Suzuki A, Katsu Y, Kobayashi M, Goto M, Handa H *et al.* Persistent gene expression in mouse vagina exposed neonatally to diethylstilbestrol. J Mol Endocrinol 2004; 32: 663-677.

10 Ghahary A, Chakrabarti S, Murphy LJ. Localization of the sites of synthesis and action of insulin-like growth factor-I in the rat uterus. Mol Endocrinol 1990; 4: 191-195.

11 Ignar-Trowbridge DM, Nelson KG, Bidwell MC, Curtis SW, Washburn TF, McLachlan JA *et al.* Coupling of dual signaling pathways: epidermal growth factor action involves the estrogen receptor. Proc Natl Acad Sci U S A 1992; 89:

4658-4662.

12 Nelson KG, Takahashi T, Bossert NL, Walmer DK, McLachlan JA. Epidermal growth factor replaces estrogen in the stimulation of female genital-tract growth and differentiation. Proc Natl Acad Sci U S A 1991; 88: 21-25.

13 Daikoku T, Hirota Y, Tranguch S, Joshi AR, DeMayo FJ, Lydon JP *et al.* Conditional loss of uterine Pten unfailingly and rapidly induces endometrial cancer in mice. Cancer Res 2008; 68: 5619-5627.

14 Joshi A, Ellenson LH. Adenovirus mediated homozygous endometrial epithelial Pten deletion results in aggressive endometrial carcinoma. Exp Cell Res 2011; 317: 1580-1589.

15 Kim TH, Franco HL, Jung SY, Qin J, Broaddus RR, Lydon JP *et al.* The synergistic effect of Mig-6 and Pten ablation on endometrial cancer development and progression. Oncogene 2010; 29: 3770-3780.

16 Memarzadeh S, Zong Y, Janzen DM, Goldstein AS, Cheng D, Kurita T *et al.* Cell-autonomous activation of the PI3-kinase pathway initiates endometrial cancer from adult uterine epithelium. Proc Natl Acad Sci U S A 2010; 107: 17298-17303.

17 Moll R, Franke WW, Schiller DL, Geiger B, Krepler R. The catalog of human cytokeratins: patterns of expression in normal epithelia, tumors and cultured cells. Cell 1982; 31: 11-24.

18 Gimenez-Conti IB, Lynch M, Roop D, Bhowmik S, Majeski P, Conti CJ. Expression of keratins in mouse vaginal epithelium. Differentiation 1994; 56: 143-151.

19 Yang A, Schweitzer R, Sun D, Kaghad M, Walker N, Bronson RT *et al.* p63 is essential for regenerative proliferation in limb, craniofacial and epithelial development. Nature 1999; 398: 714-718.

20 Mills AA, Zheng B, Wang XJ, Vogel H, Roop DR, Bradley A. p63 is a p53 homologue required for limb and epidermal morphogenesis. Nature 1999; 398: 708-713.

21 Bodine SC, Stitt TN, Gonzalez M, Kline WO, Stover GL, Bauerlein R *et al.* Akt/mTOR pathway is a crucial regulator of skeletal muscle hypertrophy and can prevent muscle atrophy in vivo. Nat Cell Biol 2001; 3: 1014-1019.

22 Rommel C, Bodine SC, Clarke BA, Rossman R, Nunez L, Stitt TN *et al.* Mediation of IGF-1-induced skeletal myotube hypertrophy by PI(3)K/Akt/mTOR and PI(3)K/Akt/GSK3 pathways. Nat Cell Biol 2001; 3: 1009-1013.

23 Pende M, Kozma SC, Jaquet M, Oorschot V, Burcelin R, Le Marchand-Brustel Y *et al.* Hypoinsulinaemia, glucose intolerance and diminished beta-cell size in S6K1-deficient mice. Nature 2000; 408: 994-997.

24 Kurita T, Medina RT, Mills AA, Cunha GR. Role of p63 and basal cells in the prostate. Development 2004; 131: 4955-4964.

25 Lee HW, Ahn DH, Crawley SC, Li JD, Gum JR, Jr., Basbaum CB *et al.* Phorbol 12-myristate 13-acetate up-regulates the transcription of MUC2 intestinal mucin via Ras, ERK, and NF-kappa B. J Biol Chem 2002; 277: 32624-32631.

26 Li JD, Feng W, Gallup M, Kim JH, Gum J, Kim Y *et al.* Activation of NF-kappaB via a Src-dependent Ras-MAPK-pp90rsk pathway is required for Pseudomonas aeruginosa-induced mucin overproduction in epithelial cells. Proc Natl Acad Sci U S A 1998; 95: 5718-5723.

27 Vilgelm A, Lian Z, Wang H, Beauparlant SL, Klein-Szanto A, Ellenson LH *et al.* Akt-mediated phosphorylation and activation of estrogen receptor alpha is required for endometrial neoplastic transformation in Pten+/- mice. Cancer Res 2006; 66: 3375-3380.

28 Lannigan DA. Estrogen receptor phosphorylation. Steroids 2003; 68: 1-9.

29 Campbell RA, Bhat-Nakshatri P, Patel NM, Constantinidou D, Ali S, Nakshatri H. Phosphatidylinositol 3-kinase/AKT-mediated activation of estrogen receptor alpha: a new model for anti-estrogen resistance. J Biol Chem 2001; 276: 9817-9824.

30 Squarize CH, Castilho RM, Gutkind JS. Chemoprevention and treatment of experimental Cowden's disease by mTOR inhibition with rapamycin. Cancer Res 2008; 68: 7066-7072.

31 Klotz DM, Hewitt SC, Ciana P, Raviscioni M, Lindzey JK, Foley J *et al.* Requirement of estrogen receptor-alpha in insulin-like growth factor-1 (IGF-1)-induced uterine responses and in vivo evidence for IGF-1/estrogen receptor cross-talk. J Biol Chem 2002; 277: 8531-8537.

32 Joshi A, Wang H, Jiang G, Douglas W, Chan JS, Korach KS *et al.* Endometrial tumorigenesis in Pten(+/-) mice is independent of coexistence of estrogen and estrogen receptor alpha. Am J Pathol 2012; 180: 2536-2547.

33 Brake T, Lambert PF. Estrogen contributes to the onset, persistence, and malignant progression of cervical cancer in a human papillomavirus-transgenic mouse model. Proc Natl Acad Sci U S A 2005; 102: 2490-2495.

34 Ozawa S, Iguchi T, Sawada K, Ohta Y, Takasugi N, Bern HA. Postnatal vaginal

nodules induced by prenatal diethylstilbestrol treatment correlate with later development of ovary-independent vaginal and uterine changes in mice. Cancer Lett 1991; 58: 167-175.

35 Segrelles C, Moral M, Lara MF, Ruiz S, Santos M, Leis H *et al.* Molecular determinants of Akt-induced keratinocyte transformation. Oncogene 2006; 25: 1174-1185.

36 Shaw RJ, Cantley LC. Ras, PI(3)K and mTOR signalling controls tumour cell growth. Nature 2006; 441: 424-430.

37 Majumder PK, Febbo PG, Bikoff R, Berger R, Xue Q, McMahon LM *et al.* mTOR inhibition reverses Akt-dependent prostate intraepithelial neoplasia through regulation of apoptotic and HIF-1-dependent pathways. Nat Med 2004; 10: 594-601.

38 Neshat MS, Mellinghoff IK, Tran C, Stiles B, Thomas G, Petersen R *et al.* Enhanced sensitivity of PTEN-deficient tumors to inhibition of FRAP/mTOR. Proc Natl Acad Sci U S A 2001; 98: 10314-10319.

39 Platz CE, Benda JA. Female genital tract cancer. Cancer 1995; 75: 270-294.

40 Mudhar HS, Smith JH, Tidy J. Primary vaginal adenocarcinoma of intestinal type arising from an adenoma: case report and review of the literature. Int J Gynecol Pathol 2001; 20: 204-209.

41 McCluggage WG, Price JH, Dobbs SP. Primary adenocarcinoma of the vagina arising in endocervicosis. Int J Gynecol Pathol 2001; 20: 399-402.

42 Ebrahim S, Daponte A, Smith TH, Tiltman A, Guidozzi F. Primary mucinous adenocarcinoma of the vagina. Gynecol Oncol 2001; 80: 89-92.

43 Herbst AL, Ulfelder H, Poskanzer DC. Adenocarcinoma of the vagina. Association of maternal stilbestrol therapy with tumor appearance in young women. N Engl J Med 1971; 284: 878-881.

44 Tarutani M, Itami S, Okabe M, Ikawa M, Tezuka T, Yoshikawa K *et al.* Tissue-specific knockout of the mouse Pig-a gene reveals important roles for GPI-anchored proteins in skin development. Proc Natl Acad Sci U S A 1997; 94: 7400-7405.

45 Groszer M, Erickson R, Scripture-Adams DD, Lesche R, Trumpp A, Zack JA *et al.* Negative regulation of neural stem/progenitor cell proliferation by the Pten tumor suppressor gene in vivo. Science 2001; 294: 2186-2189.

Figure legend

Fig. 1. Epithelium-specific deletion of *Pten* in mouse vagina. Pten is predominantly expressed in the basal cells in the E2-administrated control mouse vagina (A), whereas Pten is exclusively expressed in the suprabasal cells in the control OVX mice (B). In both E2-administarated and OVX *Pten* CKO mouse vagina, Pten expression is not detected in the epithelium (C, D). Scale bar: 100 μm.

Fig. 2. Effect of epithelial cell-specific inactivation of Pten on the mouse vagina. The vaginal epithelium of 8-week-old ovariectomized (OVX) control (A) and *Pten* CKO mice (B). Some parts of the *Pten* CKO vagina exhibit severe hyperplasic phenotypes with multiple abnormal gland-like pits (B'). PAS (C, D) and Alcian blue staining (E, F) indicate mucin production in the control (C, E) and *Pten* CKO vagina (D, F). E2 administration induces stratification and keratinized differentiation in the control (G) and *Pten* CKO mice (H). The epithelium in the *Pten* CKO mice administrated with E2 is thicker than that of controls (I). The recurring abnormal phenotypes of vagina in *Pten* CKO mice at 2 weeks after the last E2 administration (J; n=4). Prolonged E2 exposure results in papillomatosis, invagination of the vaginal epithelium into underlying stroma in the CKO mice (K, L; n=4). Scale bar: 100 μm.

Fig. 3. Expression pattern of cell differentiation marker in mouse vagina. Immunohistochemical staining for CK14 (A, B, I, J), CK1 (C, D, K, L), CK8 (E, F, M, N) and p63 (G, H, O, P). In OVX *Pten* CKO mice, an undifferentiating cell marker CK8 is expressed but a stratified and squamous differentiating cell marker CK1 is not (C-F), suggesting undifferentiation status of the epithelia. p63 expression is only expressed in

628 the basal layers of OVX control whereas some cells away from basal layer are also
629 positive in the OVX *Pten* CKO mice (G, H). p63 expression area appeared to be
630 extended to the upper layer upon E2 administration in the *Pten* CKO mouse (O, P).
631 Scale bar: 100 μm.
632
633 **Fig. 4.** *Pten* CKO leads to cell proliferation but not contribute to epithelial cell survival
634 in mouse vagina. BrdU immunostaining in control (A, C) and *Pten* CKO mouse vagina
635 (B, D). Note that BrdU positive cells in the upper layer of the OVX K5Cre;$Pten^{f/f}$ mice
636 (red arrowheads in panel B). Black arrowheads indicate normal cell proliferation in the
637 basal layer. Proliferation indices in the OVX *Pten* CKO mouse vagina were higher than
638 those of OVX controls (E). TUNEL assay indicates *Pten* mutation dose not influence
639 cell apoptosis in the vaginal epithelium (F-H). Black arrowheads indicate apoptotic cells.
640 Scale bar: 100 μm.
641
642 **Fig. 5.** mTOR activation is associated with hyperplasia in mouse vagina. Activation
643 status of Akt and mTOR (A). In addition to Akt, mTOR in the mutants show significant
644 increase of phosphorylation when calculated with Image J program (B). Rapamycin
645 administration can partially rescue the hyperplasic phenotype of *Pten* CKO mice, but
646 remains mucous production (C-F; n=5). The level of cell proliferation in the mutant is
647 significant reduced by rapamycin treatment (G). Rapamycin treatment did not influence
648 on the phosphorylation levels of Akt (H). Scale bar: 100 μm.
649
650 **Fig. 6.** Conditional *Pten* deletion results in MAPK and ERα phosphorylation.
651 Phosphorylated MEK and ERK1/2 were detected in the suprabasal cells in the mutants

652 (A-D). Activated MAPK remains in the *Pten* CKO mice administrated with rapamycin
653 (E, F). ERα protein was similarly expressed in both control and *Pten* CKO mouse
654 vagina (G, H), whereas phosphorylated ERα was detected only in the *Pten* CKO mice
655 (I). Expression profiles of growth factor mRNAs in OVX control and *Pten* CKO mouse
656 vagina (J). Scale bar: 100 μm.
657
658 **Fig. 7.** Estrogen-dependent localization of phosphorylated Akt expression in mouse
659 vagina.
660 Pten is mainly expressed in the basal cells in stratified and squamous epithelia in
661 epidermis of the skin (A), tongue (B), esophagus (C) and forestomach (D) of control
662 mice (Note no such signals in the *Pten* CKO mice; A'-D'). In the *Pten* CKO mice,
663 phospho-Akt expression is similarly detected in these tissues (E-H). Phospho-Akt
664 expression in the control mice is not prominent (E'-H'). Phospho-Akt is predominantly
665 expressed in the basal to suprabasal epithelial cells in the E2-administrated control
666 mouse vagina (I). In the *Pten* CKO mice, the phosphorylated Akt expression is
667 augmented (J). Akt is not phosphorylated in the absence of estrogen in the control mice
668 (K). In the OVX *Pten* CKO mouse vagina, phosphorylated Akt is evident in the
669 suprabasal epithelial cells (sbc), but not in the basal epithelial cells (bc) (L). See also
670 Fig. 1 for Pten expression. Dotted lines indicate basal layer of the epithelium. Scale bar:
671 100 μm.
672
673 **Fig. 8.** A possible scheme depicting Pten expression and its regulation of homeostasis
674 for mouse vagina in the absence (A) and presence of estrogen (B).
675

Fig. S1. Phenotypes of stratified and squamous epithelium in the *Pten* CKO mice. In the CKO mice, hyperplasia and keratosis was observed in the epidermis of skin, tongue, esophagus and forestomach.

Fig. S2. Vaginal epithelial cell-specific activation of Cre recombinase is confirmed by Rosa reporter (*K5Cre/+;R26R*^{eYFP}) mice at 8 weeks of age (A, B). Dotted line indicate basal layer of the epithelium.

Fig. S3. The phenotypes of vaginae in intact (without OVX surgery) *Pten* CKO mice. In control mice, normal estrous cycle is observed (A, B), however, vaginal smears in the *Pten* CKO mice consist of mucus and no keratinocytes (C). Histology of the vagina resembles those of the OVX *Pten* CKO mice (D, see also in Fig. 1B), suggesting a lack or very low levels of E2 production in the mutants. Ovary contains various stages of follicles and corpora lutea in controls (E), however, ovary of *Pten* CKO mouse exhibits no corpora lutea although follicles grow at mature stage (F). We thus suspected defects in the hypothalamus-pituitary axis, and the following experiments were performed by OVX mice.

Fig. 1

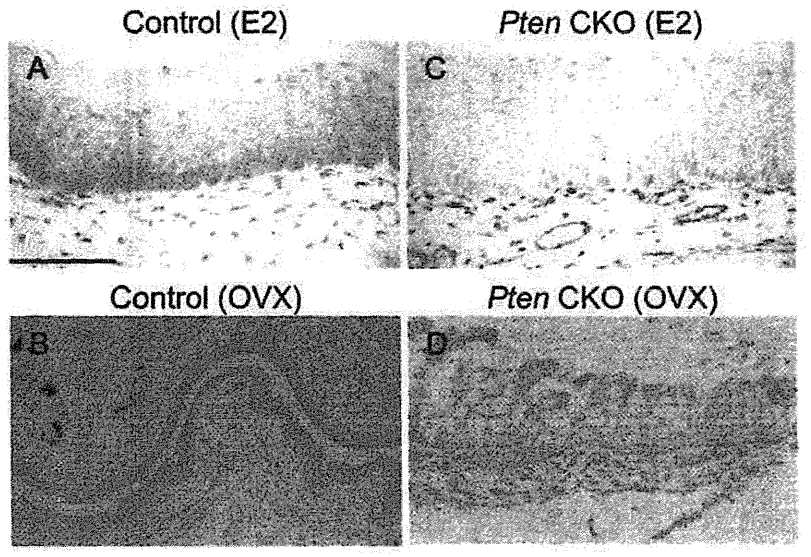

Fig. 2

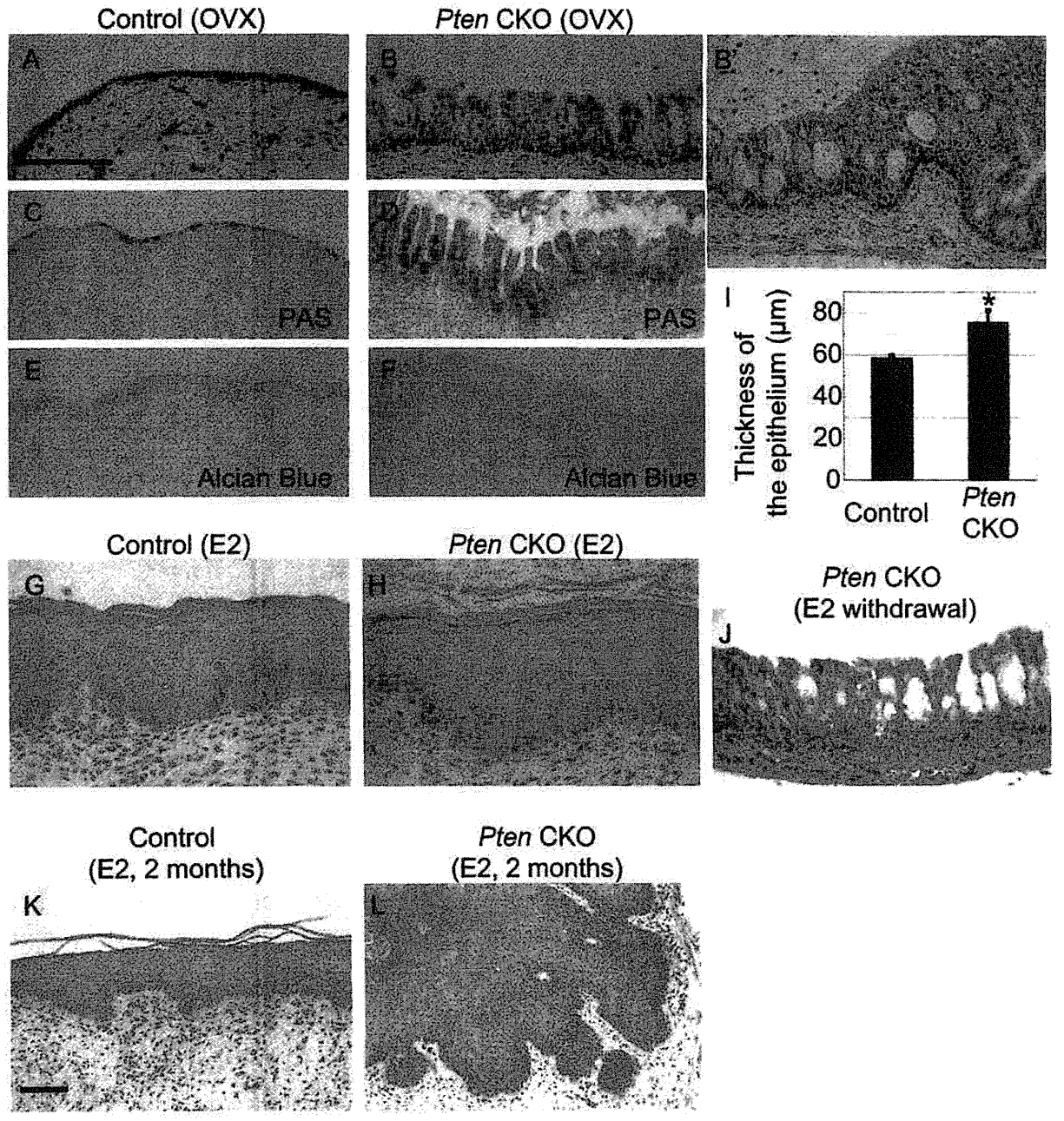
Control (OVX)
Pten CKO (OVX)
A
B
B'
C
PAS
D
PAS
E
Alcian Blue
F
Alcian Blue
I
Thickness of the epithelium (μm)
80
60
40
20
0
*
Control
Pten CKO
Control (E2)
Pten CKO (E2)
G
H
Pten CKO
(E2 withdrawal)
J
Control
(E2, 2 months)
Pten CKO
(E2, 2 months)
K
L

Fig. 3

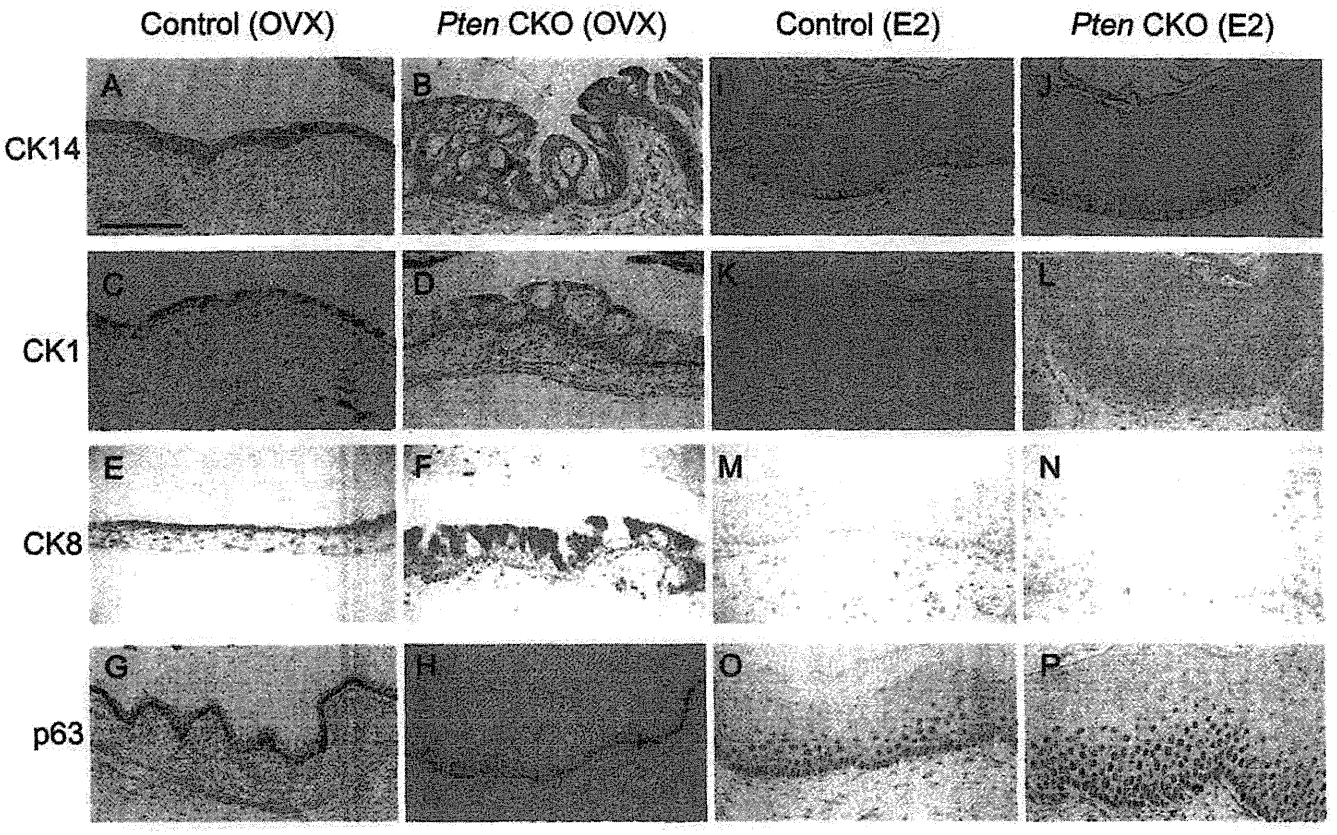
Control (OVX)
Pten CKO (OVX)
Control (E2)
Pten CKO (E2)
CK14
CK1
CK8
p63
A
B
I
J
C
D
K
L
E
F
M
N
G
H
O
P